IEEE Access
Multidisciplinary | Rapid Review | Open Access Journal

Received January 1, 2019, accepted January 12, 2019, date of publication February 20, 2019, date of current version March 18, 2019.

Digital Object Identifier 10.1109/ACCESS.2019.2894791

Novel Color Normalization Method for Hematoxylin & Eosin Stained Histopathology Images

SANTANU ROY[1], SHYAM LAL[1], (Senior Member, IEEE), AND JYOTI R. KINI[2]
[1]Electronics and Communication Department, National Institute of Technology Karnataka, Mangalore 575025, India
[2]Department of Pathology, Kasturba Medical College at Mangalore, Manipal Academy of Higher Education, Manipal 575001, India

Corresponding authors: Santanu Roy (santanuroy35@gmail.com), Shyam Lal (shyam.mtec@gmail.com), and Jyoti Kini (kinijyoti@gmail.com)

This work was supported in part by the Science and Engineering Research Board, Department of Science and Technology, Government of India, under Grant ECR/2017/000689.

ABSTRACT With the advent of computer-assisted diagnosis (CAD), the accuracy of cancer detection from histopathology images is significantly increased. However, color variation in the CAD system is inevitable due to the variability of stain concentration and manual tissue sectioning. The small variation in color may lead to the misclassification of cancer cells. Therefore, color normalization is a very much essential step prior to segmentation and classification in order to reduce the inter-variability of background color among a set of source images. In this paper, a novel color normalization method is proposed for Hematoxylin and Eosin stained histopathology images. Conventional Reinhard algorithm is modified in our proposed method by incorporating fuzzy logic. Moreover, mathematically, it is proved that our proposed method satisfies all three hypotheses of color normalization. Furthermore, several quality metrics are estimated locally for evaluating the performance of various color normalization methods. The experimental result reveals that our proposed method has outperformed all other benchmark methods.

INDEX TERMS Computer assisted diagnosis, color normalization, H & E stained histopathology image, fuzzy logic, quality metric.

I. INTRODUCTION

Histopathology refers to the pictorial examination of tissue slides under the microscope, which enables pathologists to diagnose the cancer patients in an efficient way. In recent trends, CAD has become one of the most reliable digital techniques for diagnosis and prognosis of cancer patients [1]. It is an automatic pathology diagnosis system which is employed in many hospitals in western countries. Advantage of having automatic image analysis is that it is faster than subjective pathology diagnosis and unlike subjective diagnosis it is not dependent on human psychology. Furthermore, human eyes sometimes can't detect the low-level textures or features for early cancer detection, which can be possible in case of CAD. First, histopathology slides are prepared [2], [3] by several steps like tissue collection followed by fixation, embedding, sectioning and staining. Furthermore, the slides are converted into digital images by Whole Slide Imaging (WSI) techniques [4]. These digital images are called source images throughout this paper. These source images are taken as input to a CAD system in order to detect cancerous cells with higher accuracy compared to manual cancer detection. However, CAD will not work efficiently if initially there is color variation in a set of source images due to the use of different scanners, variability of stain concentration and poor tissue sectioning. Small color variation may lead to misclassification of cancerous cells, since color is a significant feature for detecting cancer cells in histopathology images, according to our pathologist group (in Kasturba Medical College, Mangalore, India). Thus, the first step of a CAD system is color normalization which is a very much significant step in order to reduce the inter-variability of background color among a set of source images. The reason why we are focused only with the background color (not entire color), is explained in detail in section III. Moreover, in any color normalization method, a target image color should be incorporated as a standard color. This target image should be chosen by experts or pathologists and the color of target image should be transferred from target image to source image. After this

color transformation, the final image will be called as processed image, throughout this paper. A review of several color normalization methods is explored by our team in [5]. It can also be found in the literature [6]–[19].

In case of histopathology images, often staining is done by Hematoxylin and Eosin. Hematoxylin is mostly bound to the nuclei (bluish pink color) and Eosin is mostly bound to the cytoplasm (red color). However, according to Ruifrok and Johnston [10], absorption spectra of multiple stains have overlapping regions in H & E stained histopathology images. Thus, transferring color in RGB space may result undesired color mixing in the processed image, since R, G and B channels are not exactly uncorrelated. Hence, before normalizing color, this is essential to transform that image into a color space such that the (stain) channels will be kind of uncorrelated or independent. Several stain separation methods are explored by the researchers in the literature [6]–[17].

Contrast enhancement of histopathology image is only required if the images are faded due to keeping the tissue slides for more than three months, without storing it in the computer. Mostly, histopathology images have good contrast with less noise, due to the use of advanced digital slide scanners such as Olympus, Aperio, Hamamatsu etc. However, various color normalization methods may eventually reduce the contrast of the source image (e.g. Reinhard method), which is not desirable. Moreover, several color normalization methods can eliminate some of the relevant information (e.g. Stain Color Descriptor method) from the source images which is not acceptable by the pathologists (those results are shown later in section VII). Hence, color normalization should be done in such a way that it must maintain good contrast with preserving all the source information in the processed image. Based on this concept, three hypotheses of color normalization method are formulated in section III.

The main contribution of this paper is as follows. We believe that because of the unique texture property of histopathology images, mentioned in section II, global color normalization method works better than local method. That is why, we proposed a novel global method, by employing fuzzy logic, which overcomes the limitation of conventional Reinhard method. Furthermore, we prove that our proposed method satisfies all three hypothesis of color normalization both mathematically and experimentally.

The rest of the paper is organized as follows. First, unique texture property of histopathology image is presented in section II. Moreover, hypothesis of color normalization method is formulated in section III. In section IV, we explain state-of-the-art of several color normalization methods. Thereafter, limitations of conventional Reinhard method are given in section-V. In section VI, Fuzzy based modified Reinhard method is proposed in order to overcome the limitations of conventional Reinhard method. In section VII, both qualitative and quantitative results of various benchmark algorithms are compared with the same of our proposed method. Finally, we present our concluding remarks, in section VIII.

II. TEXTURE PROPERTY OF HISTOPATHOLOGY IMAGES

Texture is inherently related to the statistical (spatial) distribution of intensity values inside a local region of an image. Texture [20] can be mathematically defined as follows.

$$T = \{f(x)\}_{x \in X} \tag{1}$$

where $f(x)$ is a probability density function inside a local patch ($x \in X$) of an image.

We have found that histopathology images are having some unique texture properties which are discussed below.

A. In histopathology images, the texture property only for one feature (intensity), is approximately repeating all over the image. This kind of texture is known as periodic texture [20]. Mathematically, an image texture will be approximately periodic if

$$f(x_i) \approx f(x_j), \quad \forall i \neq j \tag{2}$$

Equation (2) implies that probability density function in any two patches (i^{th} and j^{th} window) in image are approximately same in case of periodic texture. However, the aforementioned property is not true for every size of patch. This patch size for which the texture is approximately periodic, actually depends on the autocorrelation co-efficient of the image pixel intensity values. If autocorrelation co-efficient [21] is higher, then the texture will repeat after a large patch and if the reverse is true, then texture will be periodic for a small resolution patch.

B. Empirically we have found that, for histopathology images mostly heterogeneous property (of intensity values) dominates over homogeneity property (if the small patch size is taken greater than 17×17). This implies that unlike natural images, histopathology image does not have a large region where intensity variation is approximately zero (example sky, tree, land etc.). In other words, in histopathology images, autocorrelation coefficient [21] between pixel (intensity) values is comparatively greater than that of natural images. Due to this texture property, global color normalization method or any global transformation is very much suitable for histopathology images, rather than local transformation. Moreover, autocorrelation co-efficient [21] of 50 natural images and 50 histopathology images are estimated and compared in appendix-II, in order to verify this texture property.

III. FORMULATING HYPOTHESES OF COLOR NORMALIZATION METHOD

First, some statistics of an image is introduced in this section, which will be relevant to further understand the hypothesis of color normalization.

Any image can be decomposed by its global mean and intensity variation with respect to global mean, given in

equation (3), where μ_g represents global mean and $I(x, y)$ indicates the intensity of a pixel at position (x,y).

$$I(x, y) = \mu_g [I(x, y)] + \left[I(x, y) - \mu_g(I(x, y))\right] \quad (3)$$

The first term in equation (3), is just a constant value which indicates the surrounding intensity of the image. This is significant to mention that intensity of image means intensity of its brightness as well as it can be its color intensity. The second term $(I - \mu_g(I))$ in equation (3) is very much significant as it contains all the intensity variations of the image with respect to surrounding intensity. According to our understanding, this second term contains all the significant information of an image.

Any color normalization method must satisfy the following three hypotheses, according to our understanding. Every hypothesis is explained below with proper justification. To the best of our knowledge, this is the first attempt to formulate such a mathematical hypothesis in order to evaluate the performance of any color normalization method for histopathology images.

A. CORRELATION CO-EFFICIENT

Color normalization method must preserve all the information of the source image, according to our pathologists' group. This information preservation can be measured by estimating correlation co-efficient between source image and processed image. The correlation co-efficient between two random variables measures the degree of their linear correlation [22]. Mathematically, this is the ratio of covariance between two random variables (X and Y) to the product of their individual standard deviation which is given in equation (4). The first hypothesis of color normalization method is given in equation (4).

$$\rho_{XY} = \frac{\sigma_{XY}}{\sigma_X \sigma_Y} \approx 1 \quad (4)$$

If correlation coefficient between source image (X) and processed image (Y) is exactly equal to 1, this implies that X and Y are perfectly linearly correlated. That implies,

$$Y = cX \quad (5)$$

where c is a real constant. Then mathematically, the probability density function (pdf) $f_Y(Y)$ of the processed image Y, can be expressed in terms of pdf $f_X(X)$ of the source image X, by the statistical formula [23], given by equation (6). Here X and Y are considered as random variable.

$$f_Y(Y) = \sum_{i=1}^{n} f_X(X_i) \left| \frac{dX_i}{dY} \right| \quad (6)$$

where n is the number of roots of equation (5). By applying this statistical formula (6), into the equation (5), we get the following equation (7).

$$f_Y(Y) = \frac{1}{c} f_X(X) \quad (7)$$

Equation (7) reveals that the shape of the normalized histogram (pdf) of source image will remain unchanged in the processed image, since only the magnitude of pdf is scaled by a real constant c. Hence, the correlation coefficient equals to 1, implies that all the intensity variation of source image is exactly preserved in the processed image, which is very much desirable for any color normalization method. Wang *et al.* [24] described this correlation co-efficient as a measurement of structural similarity between two grey scale images. This parameter has also been preferred as Pearson Correlation Co-efficient (PCC).

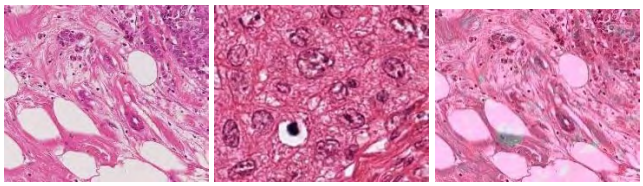

FIGURE 1. (a) Source image, (b) target image, (c) processed image.

However, some of the researchers had employed discrete entropy for measuring information preservation [25]. According to our visualization, the value of discrete entropy is just a measurement of total information in the image. It doesn't say whether that information is relevant or irrelevant. To the best of our knowledge, when someone want to extract additional information from the original image (e.g. satellite images), discrete entropy will be a kind of relevant measurement. However, in case of histopathology images, our goal is not to extract enough information, rather we want to preserve all the information of source images during the color normalization process. Hence, for the histopathology images, we believe that correlation coefficient is more realistic metric than discrete entropy for evaluating the preservation of source information.

B. GLOBAL MEAN COLOR IN COLOR SPACE

The second hypothesis of color normalization method is that in any color normalization method, global mean color (background color) of processed image should be equal to global mean color of target image. In other words, in color space ($\alpha\beta$ space),

$$\mu_{tar} \approx \mu_{proc} \quad (8)$$

where μ_{tar} is the mean color of target image, μ_{proc} is the mean color of processed image.

According to our imagination, there are two ways of transferring color from target image to source image. First way is to transfer the entire color, which is composed of background color and all the color variations with respect to mean color value, given in equation (3). If someone transfers the entire color from target image to source image, then all the color intensity variation associated with the target image will also be copied to the source image. Therefore, it will produce color artifact in the processed image shown in Fig.1c and all the color variation of source image will not be preserved by this method.

The second way, is to transfer only the background color from target image to source image, while all the source color variation with respect to mean, in equation (3), will remain same. Thus, transferring the color by this method, can actually preserve all the source color variation in the processed image and simultaneously it can reduce the inter-variability of background color among the source images. Therefore, we are considering this second way of transferring background color from target image to source image. Reinhard method and our proposed method are similar kind of color normalization method.

C. CONTRAST OF THE IMAGE

Contrast of the source image must be maintained in the processed image, since some of the color normalization methods may eventually reduce the contrast in the processed image [e.g. Reinhard method, SCD method]. This implies that contrast of the processed image (C_{proc}) should be always greater than the contrast of source image (C_{source}). The third hypothesis of color normalization is given by the equation (9).

$$C_{proc} \geq C_{source} \tag{9}$$

However, the contrast enhancement of the source image should not be unbounded. In other words, there should not be excess or over contrast enhancement, since the histopathology images are already having good contrast, according to our observation. Moreover, due to excess contrast enhancement, nuclei color might be very much darker than the conventional nuclei color (blue) which can be interpreted as a malignant tumor, according to our pathologists' group (in KMC, Mangalore). Thus, it can misclassify the cancer cells in histopathology images. Unfortunately, we didn't find any limit or maximum contrast enhancement value theoretically. That is why, we employed a fuzzy logic technique in our proposed method, in order to control the contrast enhancement.

IV. STATE-OF-THE-ART: COLOR NORMALIZAION METHOD

There are three types of color normalization method which are (A) Global color normalization (B) Stain separation by supervised method and (C) Stain separation by unsupervised methods.

A. Global color normalization method is generally performed after separating color and brightness intensity information in $l\alpha\beta$ space [26], by employing Principal Component Analysis (PCA). According to our visualization, separating color and brightness intensity is very much equivalent to stain separation method.

Histogram Specification [19] is a global color normalization method, in which source image histogram is mapped with target image histogram such that both brightness and color statistics are transferred from target image to source image. However, HS method follows Global Histogram Enhancement (GHE) which is not a linear process, according to our visualization. This method forcefully stretches the histogram of source image until it will be approximately same as the histogram of target image. Thus, it may bring undesirable artifact in the processed image.

Reinhard *et al.* [18] preferred another global color normalization method which transfers only the background color from the target image to source image with preserving all other intensity information. This algorithm was first employed for natural images by Reinhard *et al.* [18]. The main limitation of this algorithm was that the target image and source image should have exactly same kind of statistics. However, this is not the same in case of histopathology images. Because of the unique texture property of histopathology images, mentioned in section II, Reinhard algorithm is actually suitable for color normalization of histopathology images. Reinhard algorithm is further explained in depth in section V.

B. First the concept of stain separation is explained in depth in this sub-section. According to Lambert Beer's law, given in equation (10), stain concentrations are non-linearly dependent in RGB space [10]. Therefore, one has to first convert the image from RGB space to Optical Density (OD) space such that multiple stains will act linearly [10].

$$I_C = I_0 \exp(-OD_c) \tag{10}$$

where I_C is the intensity of transmitted light through histopathology slides, I_0 is the intensity of incident light on histopathology slides, OD_C is the intensity value of the image in OD space. The purpose of any stain separation method is to factorize OD space intensity value into two orthogonal matrices [10], S and D given in equation (11), such that the stain channels will be kind of independent.

$$OD_C = \log\left(\frac{I_0}{I_C}\right) = SD \tag{11}$$

where D is the stain color appearance matrix whose rows represent color basis vectors for each stains and S is the stain depth matrix whose columns represent concentration or absorption factor of each stain.

Ruifrok and Johnston [10] have proposed a novel color deconvolution method, in which stain color appearance matrix was manually estimated by measuring the relative color proportion for R, G and B channel with only single stained (Hematoxylin or Eosin only) histopathology slide. Furthermore, stain depth matrix S can be easily evaluated by taking the inverse of D and multiplied by OD space intensity values, from equation (11). However, this method requires some prior information of single stain color, which is not readily available in hospitals.

Khan *et al.* [13] proposed a novel color normalization method which is comprised of four separate methods. First, by employing Stain Color Descriptor (SCD) global method they found overall stain color. Second, a supervised color classification method i.e. Relevance Vector Machine (RVM) has been incorporated to identify the locations where each stain is present. Thereafter, color appearance matrix and

stain depth matrix are estimated from these set of classified pixels. Furthermore, a non-linear spline-based color normalization method is employed to transfer color locally from target image to source image. We believe that the SCD estimation followed by RVM to find the color appearance matrix is reliable, since it is done by a supervised learning method where single stained histopathology slides are taken as ground truth. However, due to transferring the color by a non-linear function, this algorithm can't preserve the exact shape of the source image histogram in the processed image, causing major information loss.

C. Independent Component Analysis (ICA) and Non-negative Matrix Factorization (NMF) methods both are unsupervised stain separation method which have been employed in [9] and [11]. The main advantage of unsupervised method is that there is no requirement of labeled data or ground truth of single stained histopathology image. NMF is an optimization technique which minimizes the distance between the source image and decomposed matrices (S and C), with the constraint that all co-efficient of color appearance matrix must be non-negative (i.e. $S_{i,j} \geq 0$ and $D_{i,j} \geq 0$). However, NMF method is having some problem with ambiguity and has no closed form of solution. On the other hand, ICA method assumes that each stain acts independently on histopathology slides [11], which is not always true. Therefore, this method is not practically feasible.

Macenko *et al.* [12] and McCann *et al.* [14] both of them have employed same kind of stain separation method which is based on the fact that color of each pixel in histopathology image is nothing but a linear combination of two stain vectors. The weightage of those stain vectors must be non-negative. Thus, the weightage always lies between those two stain vectors (i.e. between only Eosin and only Hematoxylin). Both of the methods tried to find a wedge of those weightage values instead of searching peaks [14]. However, this kind of method can't always estimate the right stain vectors if strong staining variation is present in histopathology slide, according to Bejnordi *et al.* [17].

In Complete Color Normalization (CCN) method, Li and Plataniotis [7] have employed both illuminance normalization and spectral normalization. Spectral normalization method comprises of two parts I) NMF based spectral estimation, II) Spectral matching. Before applying NMF, a novel Saturation Weighted (SW) statistics method has been employed which smooth out Hue histograms and converted the image to a highly saturated image. This implies that color appearance matrix is converging into a diagonal matrix. Thus, it can reduce the solution space of NMF into a unique solution. Furthermore, a unique spectral matching method is employed such that it preserves the entire stain depth matrix. However, this method couldn't preserve all the color variation of source image, since the color appearance matrix is entirely changed into a diagonal matrix, according to our visualization.

Structure Preserving Color Normalization (SPCN) method is recently proposed by Vahadane *et al.* [6]. First sparseness has been incorporated into the optimization equation of NMF, in order to reduce its solution space. Furthermore, a joint non-convex optimization problem is solved by block co-ordinate descent algorithm which is readily available in Sparse Modeling Software (SPAMS). However, computation complexity of Sparse NMF (SNMF) has considerably increased. Moreover, a structure preserving color normalization method has been employed in order to preserve the structure of the source image. According to our visualization, this structure only associates with the brightness intensity information of histopathology images, since only stain depth matrix is preserved by this method. Thus, color variation is not exactly preserved by SPCN method, similar examples are shown in section VII.

V. REINHARD METHOD

In this section, we briefly introduced the pseudo code of conventional Reinhard algorithm which is followed by its limitations.

A. PSEUDO CODE OF REINHARD METHOD

Step 1: Convert both of the source image X and target image Y from RGB space to $l\alpha\beta$ space [26].

Step 2: Do the following transformation in $l\alpha\beta$ space.

$$l_2 = \mu_g(l_1) + \left[l - \mu_g(l)\right] . * \left[\sigma_g(l_1)/\sigma_g(l)\right] \quad (12)$$

$$a_2 = \mu_g(a_1) + \left[a - \mu_g(a)\right] . * \left[\sigma_g(a_1)/\sigma_g(a)\right] \quad (13)$$

$$b_2 = \mu_g(b_1) + \left[b - \mu_g(b)\right] . * \left[\sigma_g(b_1)/\sigma_g(b)\right] \quad (14)$$

where l_2, a_2, b_2 are intensity variables of processed image in $l\alpha\beta$ space, l_1, a_1, b_1 are intensity variables of target image in $l\alpha\beta$ space and l, a, b are intensity variables of source image. μ_g indicates global mean of the image and σ_g represents global standard deviation of the image.

Step 3: Convert back the processed image Z from $l\alpha\beta$ space to RGB space.

Reinhard algorithm is a global color normalization method in which all the source intensity variation has been preserved in the processed image, since correlation co-efficient between source and processed image are found to be very much closed to 1 (shown in the table in section VII, also mathematically proved in Appendix-I). Moreover, the mean intensity of source image is replaced with the mean intensity of target image in all three channels, observed in equations (12-14). That is why, after this color transformation, global mean color (background color) of processed image is found to be very much closed to the same of target image. Thus, first two hypotheses of color normalization method are satisfied by Reinhard method. The aforementioned statement is mathematically proved in the Appendix-I. However, Reinhard method has certain limitations which are as follows.

- The background luminance of source image is not preserved in the processed image, which can be observed from the equation (12).

- When the source image has greater contrast than that of target image, then also it transfers the contrast statistics from target to source image, which may lead to lesser contrast of processed image than that of source image. Therefore, it doesn't satisfy the third hypothesis of color normalization.
- Due to transferring the mean color globally from target image to source image, it transfers the same mean color to all the pixels in the image. Thus, a large homogeneous portion, associated with white luminance in the source image, can be affected by a fade color by this method. This kind of color variation is not desirable according to Khan *et al.* [13] and Vahadane *et al.* [6]. Similar examples are given in section VII, where processed images are affected by fade color.

VI. PROPOSED COLOR NORMALIZATION METHOD

In this section, Fuzzy based Modified Reinhard (FMR) method is proposed for color normalization of H & E stained histopathology images which overcome all the limitations of Reinhard method. The detailed pseudo code of FMR method is given in this section which is followed by its physical interpretation and statistical analysis.

This is important to clarify that we have employed fuzzy logic just to control the contrast enhancement in l space and to control the color co-efficients in $\alpha\beta$ space, in order to reduce color variation. Fuzzy function is generally a mapping from a crisp set to a vague set, which makes the transformation function smoother and continuous. However, we are not interested to go back from fuzzy space to real numbers space, thus de-fuzzification is not required [27].

A. FUZZY MEMBERSHIP FUNCTION

The fuzzy membership function which we are going to employ in our proposed method, can be generalized by one single function which is given in equation (15).

$$q = \varphi_1 - (\varphi_1 - \varphi_2)/\{1 + \exp[(p - t)/(\gamma)]\} \qquad (15)$$

where q is a kind of sigmoid function whose value always lies between φ_1 and φ_2,φ_1 is the maximum value of the fuzzy function, φ_2 is the minimum value of the fuzzy function, 'p' is a parameter defined in equation (16), 't' is the crossover point or threshold value which determines the symmetricity of the function, γ is a parameter which controls the fuzziness (smoothness) of the function. Very small value of γ means the function will become very much crispy or discrete. Greater the value of γ means the function will become smoother than the previous.

The value of the parameter γ must lie between 0 to 1, When $\gamma = 1$, the fuzzy function will be tending to a straight line. In the graph in Fig.2, it is shown that how fuzzy function 's', mentioned in equation (17), changes with the value of γ. Those graphs are implemented in MATLAB 2015a.

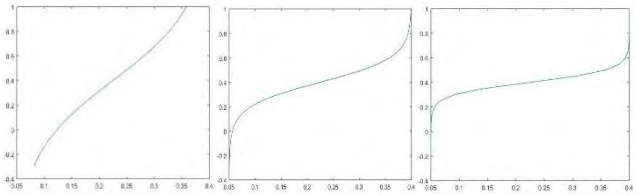

FIGURE 2. Fuzzy function 's' with (a) $\gamma = 0.5$, (b) $\gamma = 0.1$, (c) $\gamma = 0.05$.

TABLE 1. Algorithm to estimate number of pixels associated with white luminance portion.

SI No	Algorithm to estimate no of pixels associated with white luminance portion
1.	h1=0
2.	z=0
3.	for $x = 0: w1: length(x) - w1$
4.	$x = x + 1$
5.	for $y = 0: w2: length(y) - w2$
6.	$y = y + 1$
7.	$k1 = 0$
8.	for $i = 0: 1: (w1 - 1)$
9.	$k1 = k1 + 1$
10.	$k2 = 0$
11.	for $j = 0: 1: (w2 - 1)$
12.	$k2 = k2 + 1$
13.	$k = l(x + i, y + j)$
14.	$if\ (k > 0.9 * lmax)\&\&\ (lmax >= 240)$
15.	$h1 = h1 + 1$
16.	end
17.	$z = z + 1$
18.	$A(z) = l(x + i, y + j)$
19.	end
20.	end
21.	$if\ (std(A) > 0.5 * sqrt(mean(var(l))))$
22.	$h1 = h1 - 1$
23.	end
24.	end
25.	end
26.	$h = h1/(k1 * k2)$

B. ESTIMATING NUMBER OF PIXELS ASSOCIATED WITH HOMOGENEOUS WHITE LUMINANCE PORTIONS

First, the number of pixels associated with homogeneous white luminance portions are estimated locally, since the fade color effect (mentioned in section V) is directly correlated with this number of pixels. This algorithm is implemented in MATLAB 2015a, pseudo code is given in the following table 1.

h1 is the total number of pixels associated with homogeneous white luminance portion, the value of *h1* is normalized to *h* such that for any dataset, *h* will have same range of values (i.e. 0-100). The normalized factor of *h1* (i.e. *k1 x k2*k1 $*$ k2) is the window size which is same as *w1 x w2*. This is important to specify that we are looking for large (at least 35×39 patch) homogeneous region with only having white luminance in the source image and we have estimated the total number of pixels inside such regions. If intensity value of a single pixel in the source image is greater than $0.9 * lmax$ and $lmax > 240$ then only we increase the count of such pixels.

[*lmax* is the maximum intensity in l space]. But according to our understanding, that is only the count of pixels, having luminance value closed to its maximum value. Therefore, such pixels are associated with only white luminance.

However, we need to check whether these white luminance pixels are associated with homogeneous region or not, over a large patch or window. Window size *w1 x w2* (35 x 39 for breast cancer and 36 × 53 for liver cancer dataset) for both of the databases are chosen empirically. If a pixel is associated with non-homogeneous white luminance portion, then such a count should be excluded from *h1*. That is why, in this algorithm, a portion of global standard deviation of the image is employed as threshold value. If $\sigma(A) > 0.5 * \sigma_g(l)$ (i.e. inside A region, intensity variation is high enough, it is greater than half of global standard deviation of l), then that region A is detected as non-homogeneous region and simultaneously the counter value of *h1* will be decreased by 1. All these threshold values, in this algorithm are chosen empirically.

C. PROPOSED FMR METHOD

The proposed FMR method is presented in this subsection in the form of mathematical equations. Those equations will be useful to prove hypotheses. Furthermore, a flow chart of FMR method is presented in the Fig.3.

Step 1: Convert both of the source image X and target image Y from RGB space to $l\alpha\beta$ space [26].

Step 2: Calculate the parameter 'p' for every source image, which is defined in equation (16).

$$p = \frac{\sigma_g(l_1) - \sigma_g(l)}{\sigma_g(l_1)} \tag{16}$$

Step 3: Define the fuzzy function 's' in l space.

if (p>0)

$$s = 0.4 - (0.35)./\{1 + \exp[(p - 0.4)/(0.1)]\} \tag{17}$$

else

$$s = 0.05 \tag{18}$$

end

All the parameters of fuzzy function 's' are chosen empirically.

Step 4: Do the following transformation in l space. All the parameters l, l_2, μ_g were already mentioned before in section V.

$$l_2 = \mu_g(l) + \left[l - \mu_g(l)\right] . * (1 + s) \tag{19}$$

Step 5: Define the fuzzy function in color space

$$\text{Initialize } q = 0 \tag{20}$$

Store the value of h which was previously estimated in subsection B.

if (h>=20)

$$q = 0.3 - (0.25)./\{1 + \exp[(h * 0.005 - 0.1)/(0.1)]\} \tag{21}$$

end

All the parameters of fuzzy function 'q' are chosen empirically.

Step 6: Do the following transformations in $\alpha\beta$ space. All the parameters a,a_1a_2,b,b_1,b_2 and μ_g were already mentioned before in section V.

$$u = \mu_g(a_1) - \mu_g(a) \tag{22}$$

$$v = \mu_g(b_1) - \mu_g(b) \tag{23}$$

if (u>0) & (v>0)

$$a_2 = \mu_g(a_1) . * (1 - q) + \left[a - \mu_g(a)\right] \tag{24}$$

$$b_2 = \mu_g(b_1) . * (1 - q) + \left[b - \mu_g(b)\right] \tag{25}$$

else

$$a_2 = \mu_g(a_1) + \left[a - \mu_g(a)\right] \tag{26}$$

$$b_2 = \mu_g(b_1) + \left[b - \mu_g(b)\right] \tag{27}$$

end

end

Step 7: Convert l_2, a_2 and b_2 from $l\alpha\beta$ space [26] to RGB space to get the final processed image Z.

D. PHYSICAL INTERPRETATION OF PROPOSED FMR METHOD

In proposed FMR method, all the image transformations are performed in $l\alpha\beta$ space [26], like Reinhard method. First a parameter 'p' is defined in equation (16), which is directly proportional to contrast difference between a target image and source image (Here global standard deviation of image is considered to be similar to contrast of that image [24]). The value of 'p' lies between -c to 1, observed from the equation (16), where c is a real constant. Higher value of 'p' indicates that the source image has very poor contrast compared to target image. Subsequently, a fuzzy function 's' is employed in l space, which is proportional to 'p', given in equation (17). More or less the function 's' is equivalent to function 'p' which is just a measurement of how much contrast should be enhanced in the processed image. This statement is further mathematically proved in the next subsection. The maximum value of fuzzy function 's' is chosen 0.4 empirically. For example, if 'p' has a higher value 0.8, then also the value of 's' will not exceed 0.4, thus excess contrast enhancement can be controlled in the processed image by employing fuzzy function 's'. If 'p' is negative (i.e. the contrast of source image is already greater than the contrast of target image), then contrast enhancement of source image is not so necessary. At that case, our proposed method enhances the contrast a very little bit (minimum value of 's' is 0.05 or 5%) which ensures that the contrast of the processed image is always greater than that of source image, because the value of 's' is always positive. Therefore, proposed FMR method satisfies the third hypothesis of color normalization which was not true for Reinhard method. This is further proved mathematically in the next subsection.

The other parameters of 's' are chosen empirically. According to our visualization, the fuzzy function 's' is just

a mapping from a set of real numbers [− c,1] to a set of positive real numbers i.e. [0.05,0.4]. The graph of 'p' vs 's' is shown in Fig.2, for different values of γ. According to our observation, for a particular range [0.05-0.5] of values of γ, this mapping will be non-linear. We choose the value of $\gamma = 0.1$, because we prefer non-linear mapping from 'p' to 's', since it is highly correlated with human visualization. This is to clarify that we choose the mapping from 'p' to 's' to be non-linear. But it doesn't mean that our transformation function in equation (19), is non-linear. In fact, for a particular source image, the value of 's' in equation (19), is a real value which makes the transformation function linear, thus preserving the structure of source image histogram. Hence, the first hypothesis is also satisfied by our proposed FMR method. This is further mathematically proved in the next subsection. Furthermore, we observed that maximum range of values of 'p' is 0.8 for both of the datasets. Therefore, 't' is chosen 0.4 which is half of the maximum range of 'p', thus producing a symmetric fuzzy function. This is to clarify that the third hypothesis of color normalization is only dependent on single parameter 's', which is fixed for all dataset and it is always positive. Moreover, the purpose of inclusion of the parameter 's' was to avoid negative real numbers of 'p', such that the third hypothesis will be always satisfied.

One of the limitations of Reinhard method was that it doesn't preserve the background luminance of source images. To overcome this limitation, in proposed FMR method, the background luminance of processed image is exactly replaced by the background luminance of source image, given in equation (19). Therefore, background luminance of source images is exactly preserved by proposed FMR method. This is further mathematically proved in the next subsection.

Moreover, the Reinhard method has the limitation of fade color effect which was already explained in section V. This fade color effect is directly correlated with the value of 'h', which was estimated in the subsection B. A fuzzy function 'q' is employed in equation (21), which is proportional to the value of 'h'. The fade color effect happens only if the global mean color differences in $\alpha\beta$ space, i.e. 'u' and 'v' (given in equations 22-23) both are positive and the value of 'q' is higher. If $u>0$ and $v>0$, it implies that target image mean color is greater than the source image mean color, thus the transferring mean color will be higher in value. Simultaneously, if the value of 'q' is higher, this implies that there is a higher chance that the large white luminance portion is getting affected by a fade color (or, mean color). At that case, we are transferring less mean color [i.e. *(1-q)* times the target mean color], given in the equations (24-25), such that fade color effect will be less. The maximum value of 'q' is chosen 0.3 empirically given in equation (21), this implies that minimum 70 percent of mean color we always transfer from target image to source image. The threshold value for h is chosen 20 empirically. If $h<20$, that means homogeneous white luminance portion is less in the image and consequently, $q=0$. Therefore, at that case, we transfer the total mean color of the target image to the processed image, given in equations (26-27). This implies, the mean color difference between target image and processed image will be closed to zero, which is desirable for color normalization method. Hence, our proposed method satisfies the second hypothesis conditionally (i.e. it's true if $h<20$). This is further mathematically proved in the statistical analysis part. Moreover, in both α space and β space, we preserve the exact color variation of source image in the processed image. It can be observed from the equations (24-27). Therefore, colorfulness of the source image and the processed image will be approximately same, by proposed FMR method.

This is significant to clarify that this fade color effect, is depending on various parameters (like threshold values, window size) mentioned in our algorithm. However, our aim was never to remove this fade color effect completely from the processed image. White luminance homogeneous portions present in the source image, can never be perfectly preserved by proposed method, since we are globally transferring the mean color to all the pixels in the processed image. However, we just tried to reduce the fade color effect at a certain level, in order to increase the inter-color variability among several tissues present in histopathology images and consequently, at the next step of segmentation those several tissues can be easily delineated. This is to clarify that those white luminance homogeneous portions are mostly comprised of fat or lipid. Therefore, they have no important information regarding cancer cells and should be eliminated after segmentation. Thus, if those portions are slightly affected by a fade color in our proposed method, this won't have any consequences in the final result of cancer classification. On the other hand, the second hypothesis of color normalization method is not directly correlated with those parameters. It is only directly correlated with φ_1 and φ_2 i.e. the maximum and minimum values of fuzzy function 'q'. Since, those ($\varphi_1 = 0.3$ and $\varphi_2 = 0.05$) values are fixed over all databases, the performance of proposed FMR color normalization method will not be fluctuating over various databases.

E. STATISTICAL ANALYSIS OF PROPOSED FMR METHOD

A statistical analysis of proposed FMR method is presented in this subsection.

From the theory of statistics [23], we know that

$$\sigma^2(cX + d) = c^2\sigma^2(X) \tag{28}$$

where X is a random variable, $\sigma^2(X)$ is the Variance of X, 'c' and 'd' are real constants.

By taking global variance both side in equation (19) and by employing the statistical formula given in equation (28), we get

$$\sigma_g^2(l_2) = \sigma_g^2(l).*(1+s)^2 \tag{29}$$

or,

$$\sigma_g(l_2) = \sigma_g(l).*(1+s) \tag{30}$$

By taking the global mean both side in equation (19), we get

$$\mu_g(l_2) = \mu_g\left[\mu_g(l)\right] + \left[\mu_g(l) - \mu_g(\mu_g(l))\right].*(1+s) \quad (31)$$

Now, $\mu_g\left[\mu_g(l)\right] = \mu_g(l)$, since $\mu_g(l)$ is a real constant.

Therefore,

$$\mu_g(l_2) = \mu_g(l) \quad (32)$$

From the equation (32), we can say that global mean intensity or background luminance of processed image is exactly same as the background luminance of source image. Thus, background luminance of source image has been exactly preserved in proposed FMR method. Therefore, first limitation of Reinhard method is resolved in the proposed FMR method.

According to the contrast definition introduced by Mukherjee and Mitra [29], contrast of an image is given by the following equation (33), where σ is standard deviation of intensity values and μ is mean intensity or surrounding intensity.

$$C = \sigma/\mu \quad (33)$$

Similarly, global contrast of the processed image C_2 in l space can be defined by the following equation (34).

$$C_2 = \frac{\sigma_g(l_2)}{\mu_g(l_2)} \quad (34)$$

By putting the value from equation (30) and (32) into equation (34), we get,

$$C_2 = \frac{\sigma_g(l)}{\mu_g(l)}.*(1+s) \quad (35)$$

From equation (35), we can conclude that the contrast of the processed image is *(1+s)* times the contrast of source image. For a particular source image, '*s*' is having only real positive value, thus equation (35) reveals that the contrast of processed image is always greater than that of source image. Hence, third hypothesis of color normalization has been satisfied by the proposed FMR method. Moreover, equation (35), reveals that '*s*' is the measure of how much contrast is enhanced in the processed image. For example, if the value of '*s*' is 0.3, equation (35) implies that the contrast of the processed image is enhanced by 30 percent.

Now, covariance between processed image and source image in l space is given by the equation (36), from covariance definition.

$$\sigma_{ll_2} = \frac{1}{MN}\sum_{i=1}^{M}\sum_{j=1}^{N}\left[l_{2i} - \mu_g(l_{2i})\right]\cdot*\left[l_j - \mu_g(l_j)\right] \quad (36)$$

where M x N is the image size in l space. Putting the value from equation (19) and (32), in equation (36) we get,

$$\sigma_{ll_2} = \frac{1}{MN}\sum_{i=1}^{M}\sum_{j=1}^{N}\left[l_i - \mu_g(l_i)\right]^2.*(1+s) \quad (37)$$

or,

$$\sigma_{ll_2} = \sigma_g^2(l).*(1+s) \quad (38)$$

Correlation coefficient between source image and processed image in l space is given by

$$\delta = \frac{\sigma_{ll_2}}{\sigma_g(l).\sigma_g(l_2)} \quad (39)$$

Substituting the value from equation (30) and (38) into equation (39), we can get

$$\delta = 1 \quad (40)$$

Hence, it is proved that correlation coefficient between source image and processed image in l space is exactly equal to 1, in proposed FMR method. Moreover, it is significant to observe from equation (40) that, this correlation coefficient doesn't depend on any other parameter, employed in our algorithm. Thus, we can conclude that in l space, the first hypothesis is always satisfied by proposed FMR method.

Similarly, in $\alpha\beta$ space, it can be proved that proposed FMR method satisfies three of the hypotheses.

Case-I: if there is no fade color effect (if *h<20, q=0*)

By taking global variance both side in the equation (26) and by employing the equation (28), we get

$$\sigma_g^2(a_2) = \sigma_g^2(a) \quad (41)$$

or,

$$\sigma_g(a_2) = \sigma_g(a) \quad (42)$$

Similarly,

$$\sigma_g(b_2) = \sigma_g(b) \quad (43)$$

Taking global mean both side in equation (26), we get

$$\mu_g(a_2) = \mu_g\left[\mu_g(a_1)\right] + \left[\mu_g(a) - \mu_g(\mu_g(a))\right] \quad (44)$$

or,

$$\mu_g(a_2) = \mu_g(a_1) \quad (45)$$

Similarly,

$$\mu_g(b_2) = \mu_g(b_1) \quad (46)$$

Equations (45) and (46) reveals that the mean color of processed image is exactly equal to the mean color of target image. Hence, our proposed FMR method satisfies the second hypothesis conditionally i.e. if *h<20*.

Now for the covariance between processed image and source image, substituting value from equations (26) and (45) in covariance equation of α space, we get

$$\sigma_{aa_2} = \frac{1}{MN}\sum_{i=1}^{M}\sum_{j=1}^{N}\left[a_i - \mu_g(a_i)\right]^2 \quad (47)$$

or,

$$\sigma_{aa_2} = \sigma_g^2(a) \quad (48)$$

Now Pearson Correlation coefficient between source image and processed image in α space is given by equation (49).

$$\delta = \frac{\sigma_{aa_2}}{\sigma_g(a).\sigma_g(a_2)} \quad (49)$$

Substituting the values from equation (42) and equation (48), into equation (49), we get,

Or,

$$\delta = 1 \tag{50}$$

Similarly, it can be proved in β space also. Thus, in $\alpha\beta$ space it is proved that correlation co-efficient between processed image and source image is exactly equal to 1, which is not dependent on any variable. Therefore, our proposed FMR method always satisfies the first hypothesis in $\alpha\beta$ space. Hence, our proposed FMR method is capable to preserve all the color variation of source image in the processed image.

Case-II: If there is fade color effect (i.e. $h>=20$, $u>0$, $v>0$)

By following the exactly same procedure as case-I, we can get the following equations for case-II in $\alpha\beta$ space.

$$\sigma_g(a_2) = \sigma_g(a) \tag{51}$$
$$\sigma_g(b_2) = \sigma_g(b) \tag{52}$$
$$\mu_g(a_2) = \mu_g(a_1).*(1-q) \tag{53}$$
$$\mu_g(b_2) = \mu_g(b_1).*(1-q) \tag{54}$$

Equations (53) and (54) reveals that a portion of mean color of target image is transferred to processed image and that portion is directly correlated to fuzzy function 'q'. Thus, second hypothesis of color normalization is partially satisfied in case-II. However, maximum value of 'q' is chosen very less (i.e. 0.3) and the number of images with $h>=20$ is also very less in both of the databases. Thus, mean color of processed image is found very much closed to mean color of target image by FMR method.

For the correlation co-efficient, the proof is exactly same as the case-I.

Hence, it is proved that our proposed FMR method satisfies all three hypotheses of color normalization. Although, here we do kind of global estimation, it is quite amazing that all those results are exactly correlated with the local estimation. Local metric estimation is further discussed in the next section.

VII. EXPERIMENTAL RESULTS AND ANALYSIS

In this section, result of the proposed FMR method is compared with other existing color normalization methods such as Reinhard method [18], Macenko method [12], SCD method [13], CCN method [7], and SPCN method [6]. All the aforementioned methods were implemented and simulated with MATLAB 2015a, running on an Intel®Core ™ i3 PC with 2.00 GHz CPU and 8 GB RAM. For experimentation, test colon and breast cancer histopathology images are taken from publicly available databases [13] and [28] respectively. From each of the database, 100 number of images are taken for experimentation. Visual results of several color normalization algorithm are shown in Fig.4 and Fig.5.

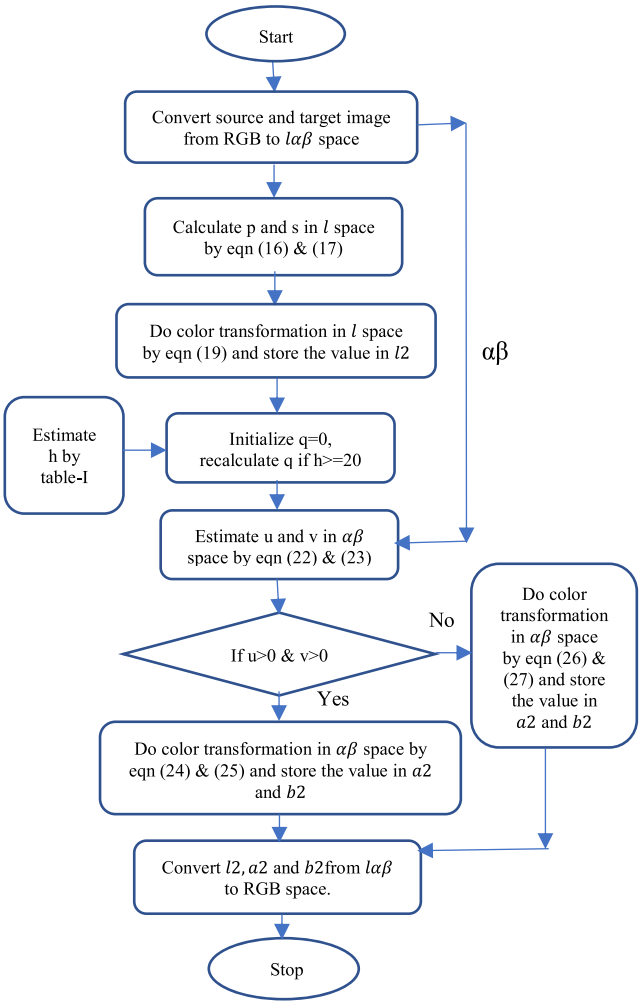

FIGURE 3. Flow chart of FMR color normalization method.

A. QUALITY METRICS FOR HISTOPATHOLOGY IMAGES

Conventional quality metrics (e.g. Full reference metric) are not suitable for histopathology images, since the ground truth of histopathology image is not available. In fact, the ground truth is lost after the staining process, since there was color variation during staining. However, we assume that brightness intensity (gray-scale) information is entirely preserved in the source image after staining process. Thus, that grey-scale information can be extracted from the source images. The color information can be extracted from the target image, which is preferred by pathologists. Therefore, quality of histopathology images can be evaluated by a Reduced Reference metric, where we are extracting significant information of ground truth from source image and target image. This work is inspired from [30]. However, we didn't choose exactly same metrics as [30]. The reason behind choosing those new metrics have already been explained in section III.

The following quality metrics are estimated locally. The mathematical expressions of those metrics are given below.

1. Structural similarity between source image (X) and processed image (Y) is measured by Pearson Correlation

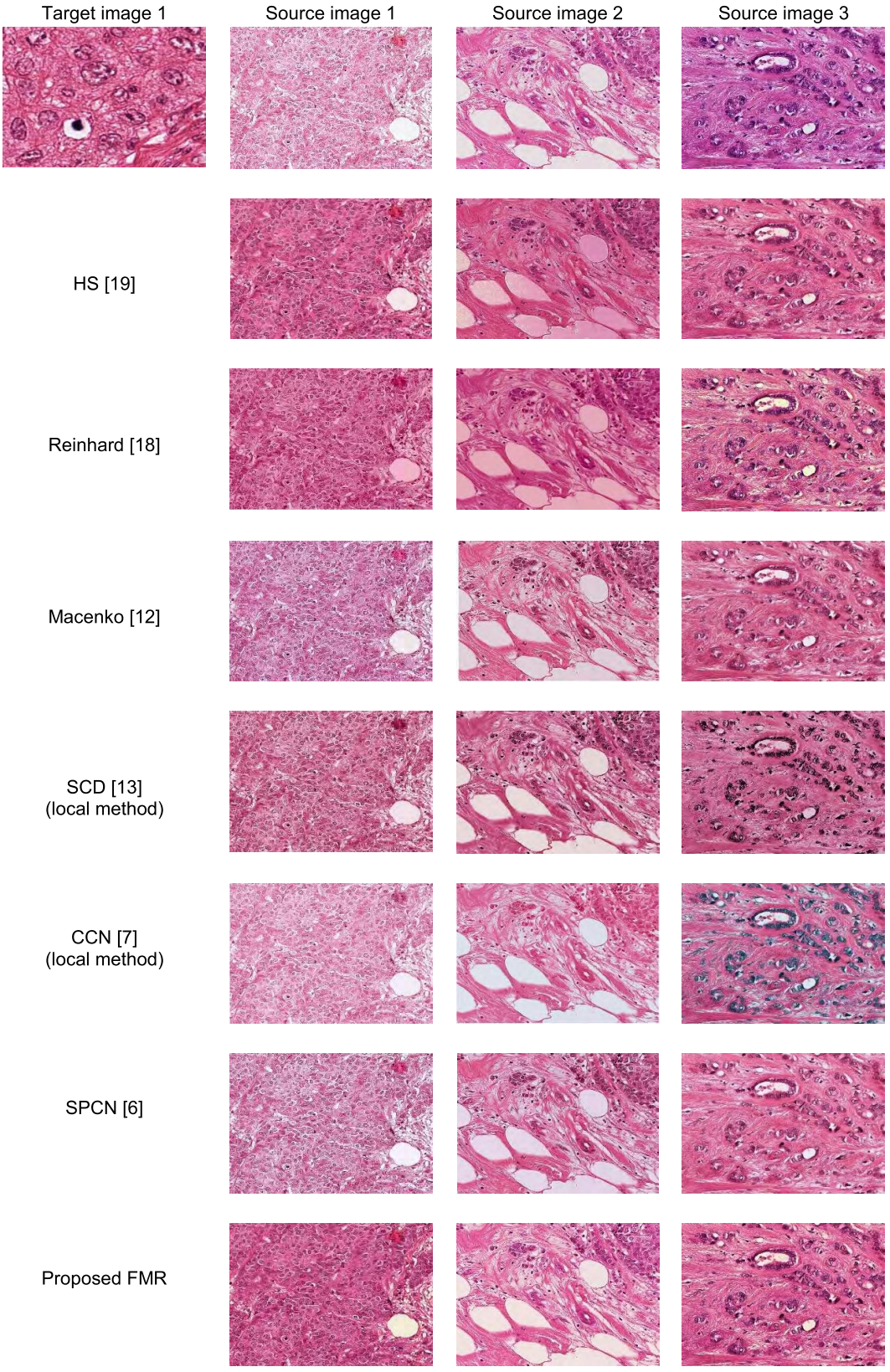

FIGURE 4. Comparison of various color normalization methods for breast cancer histopathology image. First column represents the normalized image for source image1. The second and third column represents normalized image for source image2 and source image 3 respectively.

Co-efficient (PCC) and Structural Similarity Index Metric (SSIM) [24].

$$\rho_{XY} = \frac{1}{W}\sum_{i=1}^{W}\frac{\sigma_{X_iY_i}}{\sigma_{X_i}\sigma_{Y_i}} \tag{55}$$

$$SSIM(X,Y) = \frac{(2\mu_X\mu_Y + k_1).(2\sigma_{XY} + k_2)}{(\mu_X^2 + \mu_Y^2 + k_1).(\sigma_X^2 + \sigma_Y^2 + k_2)} \tag{56}$$

$$MSSIM(X,Y) = \frac{1}{W}\sum_{i=1}^{W} SSIM(X_i, Y_i) \tag{57}$$

where X_i and Y_i are image contents at local i^{th} window, W is the total no. of window in image. MSSIM is the mean SSIM, σ_{XY} is the covariance between source image and processed image, σ_X is the standard deviation of X, μ_X is the mean value of X. Both of the value of k_1 and k_2 are in the order of 0.01.

2. Absolute Mean Color Error (AMCE) in both α space and β space are given in equations (58) and (59) respectively, where μ indicates local mean. $\alpha_i(tar)$ is the target image content at local i^{th} window in α space and $\alpha_i(proc)$ is the processed image content at local i^{th} window in α space, W is the total no of windows.

$$AMCE_\alpha = \left|\frac{1}{W}\sum_{i=1}^{W}\mu(\alpha_i(tar)) - \frac{1}{W}\sum_{i=1}^{W}\mu(\alpha_i(proc))\right| \tag{58}$$

$$AMCE_\beta = \left|\frac{1}{W}\sum_{i=1}^{W}\mu(\beta_i(tar)) - \frac{1}{W}\sum_{i=1}^{W}\mu(\beta_i(proc))\right| \tag{59}$$

The inclusion of AMCE metric is very much significant which actually enables us to measure the background color variation in the processed image, with respect to the target image.

3. Contrast Difference (CD) between processed image and source image can be measured by the following mathematical equation (60), where $\sigma(Y_i)$ and $\sigma(X_i)$ are the standard deviation of processed image and source image respectively, at i^{th} window.μ is the mean value, W is the total no of windows. The definition is inspired from [29].

$$CD(Y,X) = \frac{1}{W}\sum_{i=1}^{W}\frac{\sigma(Y_i)}{\mu(Y_i)} - \frac{1}{W}\sum_{i=1}^{W}\frac{\sigma(X_i)}{\mu(X_i)} \tag{60}$$

To satisfy the hypotheses of color normalization, mentioned in section III, the following must be true.

- PCC or MSSIM value should be very much closed to 1.
- AMCE value both in α space and β space should be closed to zero.
- CD value should have positive sign.

The window size to compute quality metric is taken 18×25 and 20×23 for colon cancer and breast cancer datasets respectively. This window size should be dependent on the entire image size and they must be chosen optimally such that the number of zero padding will be minimum. All the hypotheses (except third) of color normalization can be verified by the table 2 and table 3 which are given below. However, mean values of those quality metrics don't always reflect the actual statistics. That is why, a box plot [31] is introduced in Fig.6, for only breast cancer data set (for a set of 100 images only) which shows how the data points are varying with respect to its mean value. For third hypothesis, only the sign of CD matters, its mean value is not important. Therefore, its value is not presented in table 2 or table 3. Rather, it can be visualized in the box plots, shown in fig.6d.

TABLE 2. Mean values of quality metrics of 100 breast cancer histopathology images for various color normalization methods.

Color Normalization Approach	PCC	MSSIM	AMCE α	AMCE β	CPU Time (sec)
HS [18]	0.9835	0.9021	0.04	0.06	2.25
Reinhard [17]	0.9976	0.9740	**3.5 e^{-14}**	**1.0 e^{-14}**	**2.2**
Macenko [12]	0.9940	0.9731	1.96	2.41	5.0
SCD [13]	0.8640	0.7963	1.17	2.32	256
CCN [7]	0.9490	0.8910	3.26	4.27	22.5
SPCN [6]	0.9910	0.9671	1.08	2.35	360
Proposed FMR	**0.9998**	**0.9939**	0.42	0.89	17

TABLE 3. Mean values of quality metrics of 100 colon cancer histopathology images for various color normalization methods.

Color Normalization Approach	PCC	MSSIM	AMCE α	AMCE β	CPU Time (sec)
HS [18]	0.9910	0.9279	0.36	0.05	1.2
Reinhard [17]	0.9980	0.9680	**1.5 e^{-14}**	**2.1 e^{-14}**	**1**
Macenko [12]	0.9560	0.8659	28.3	9.53	2.25
SCD [13]	0.9041	0.8318	3.79	4.54	93
CCN [7]	0.9783	0.9699	4.69	0.925	9.5
SPCN [6]	0.9780	0.9507	3.96	0.39	120
Proposed FMR	**0.9988**	**0.9879**	0.47	0.06	3.0

B. RESULT EVALUATION AND COMPARISONS

From Fig.4 and Fig.5, it can be visualized that Reinhard method and histogram specification method don't preserve the white luminance part in the processed image.

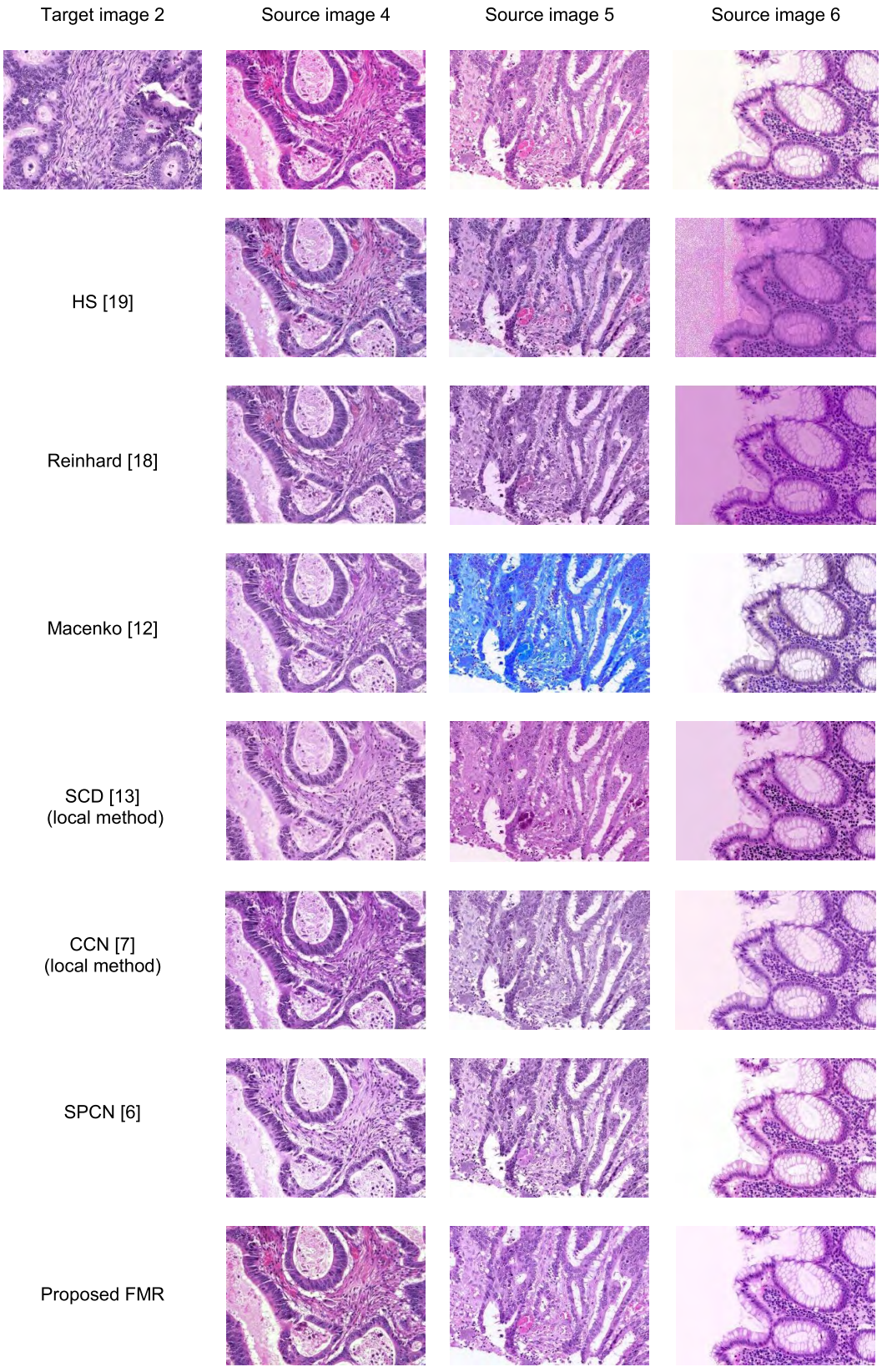

FIGURE 5. Comparison of various color normalization methods for colon cancer histopathology image. First column represents the normalized image for source image 4. The second and third column represents normalized image for source image5 and source image 6 respectively.

However, both of the methods are capable of preserving all the structural information of source image which is visualized in Fig.4 and Fig.5 and also it can be observed from the table 2, table 3 and Fig.6a. Therefore, both of the methods satisfy the first hypothesis. However, they do not satisfy the third hypothesis which can be observed from Fig.6d. Furthermore, in both of the methods, the mean of AMCE is found very much closed to 0, given in table 2 and table 3, thus they also satisfy the second hypothesis.

From Fig.5, it is visible that Macenko method doesn't transfer the right color from target image to processed image. In colon dataset it has been found that the mean value of AMCE is 28.3 in α space and 9.53 in β space, given in table 3, which are very much deviating from zero. From Fig.4 and Fig.5, it can be visualized that SCD method doesn't preserve all the source information in processed image. In fact, the loss of information in this method is greater than other benchmark methods. MSSIM is found 0.79 and 0.83 for breast and colon dataset respectively, given in table 2 and table 3. Also, PCC value is very much deviating from 1, which can be observed from Fig.6a. Thus, SCD method doesn't satisfy the first hypothesis.

From Fig.4 and Fig.5, it can be visualized that in CCN method, the white luminance part of source image is exactly preserved in their processed image. However, color information of source image is not exactly preserved by this algorithm which can be visualized in Fig.4. Thus, PCC and MSSIM are deviating from the value of 1 in case of breast cancer dataset, given in table 2. Moreover, in breast cancer dataset sometimes this method brings undesired color artifacts, because Saturated Weighted Statistics (SWS) is not exactly a linear method, according to our visualization. Furthermore, in case of breast cancer dataset, mean of AMCE is very much deviating from 0. This can also be observed from Fig.6b and Fig.6c.

We found only SPCN method a decent existing color normalization method which has desirable quality metric values, given in table 2 and table 3. From Fig.4 and Fig.5, it can be visualized that all the structural information of source image is preserved in the processed image, while transferring right color from target image to processed image. However, all the color variation of source image is not exactly preserved in the processed image, which can be seen in Fig.5, for source image 4 and source image 5. PCC and MSSIM in this method are better than CCN method, found in table 2, but still they are somehow deviating from 1. Therefore, there is a chance of improvement of getting better PCC or MSSIM. Another big disadvantage of this method is that it has large computation complexity, mentioned in table 2 and table 3.

Proposed FMR method is employed to overcome all the limitations of conventional Reinhard method. The qualitative and quantitative results reveal that our proposed FMR method outperforms all other benchmark color normalization methods. In table 2 and table 3, it is found that FMR method has the best metric values compared to recent existing methods. It has correlation co-efficient and MSSIM value both very closed to 1, this implies that it preserves all the source information in the processed image. Subsequently, it can also be visualized from the boxplot of PCC, in Fig.6a. Proposed FMR method

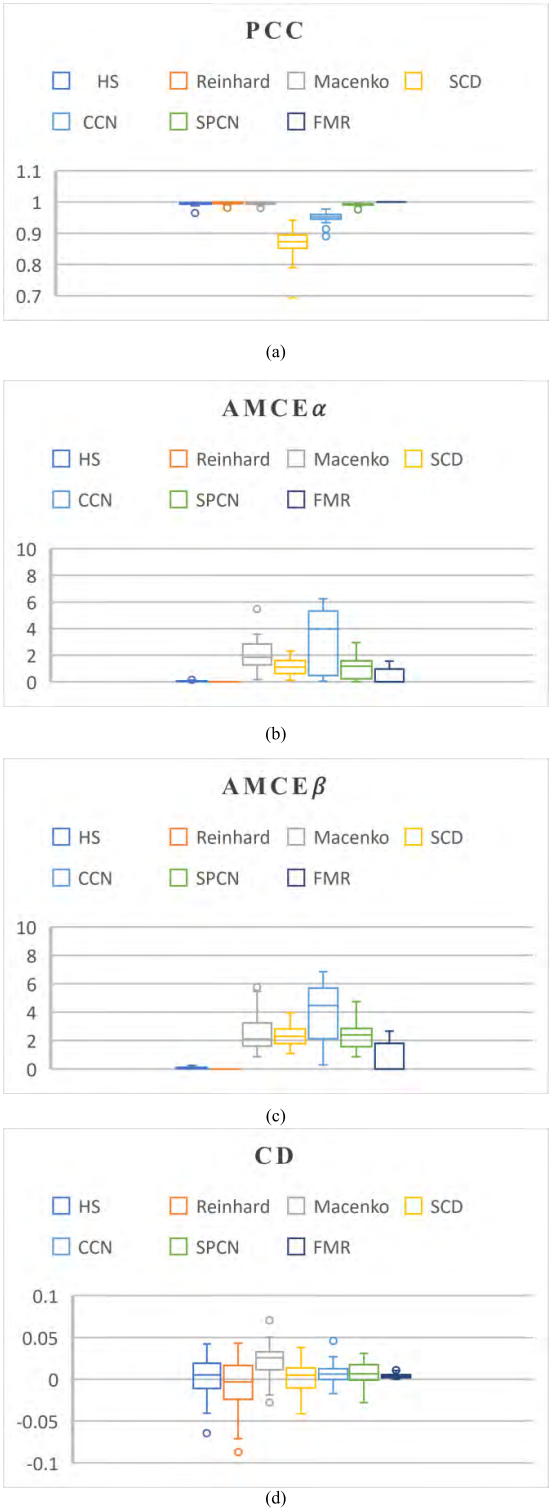

FIGURE 6. **(a) Box plot of PCC for several color normalization methods. (b) Box plot of AMCEα for several color normalization methods. (c) Box plot of AMCEβ for several color normalization methods. (d) Box plot of CD for several color normalization methods.**

has the least width in PCC boxplot, which implies that the variation of PCC value is the least in FMR method and overall PCC value is very much closed to 1. In Fig.4 and Fig.5, it can be clearly observed that proposed FMR method has preserved the white luminance part of source image better than Reinhard method and HS method. However, due to the inclusion of fuzzy functions, AMCE metric values in FMR method is slightly deviating from zero, given in table 2 and table 3 and simultaneously it can also be observed from Fig.6b and Fig.6c. But still this AMCE value for proposed FMR method is lesser than other existing algorithms except Reinhard method and HS method. Moreover, from the boxplot diagram in Fig.6d, it is observed that CD value is always positive in proposed FMR method and it has the least width in CD boxplot which is desirable. Therefore, our proposed method satisfies the third hypothesis which was not true in Reinhard method. Furthermore, the main advantage of our proposed method is that it has very much less computation complexity compared to recent existing local methods, which are mentioned in table 2 and table 3.

Correlation co-efficient, mean color difference, contrast of the image all those statistics of the processed image were mathematically derived in the statistical analysis part, which is the backbone of this research paper. However, all those statistics are estimated globally, thus one may raise a question what is the guarantee that those global estimations will be same as local estimation. Because of the unique texture properties of histopathology images (mentioned in section II), we have found that those global estimations are exactly correlated with local metric estimation, compared from table 2 and table 3. For example, in our proposed FMR method, mathematically we have proved that correlation co-efficient equals to 1 and we have found that mean value of PCC are 0.9998 and 0.9988 for breast and colon cancer database respectively, which are very much closed to 1. Furthermore, statistically we have proved that in FMR method, contrast of the processed image is always greater than that of source image. We have found the Contrast Difference (CD) value is always positive, shown in the box plot in Fig.6d. Hence, we can conclude that our statistical analysis is perfectly correlated with the quality metric evaluation.

VIII. CONCLUSION

In this paper, a global color normalization method was proposed for histopathology images. Earlier global color normalization methods (e.g. HS method, Reinhard method) were fraught with the fade color effect, appeared in the white luminance portions of the image. Also, in case of Reinhard method, the contrast of the processed image sometimes found lesser than that of source image, which is undesirable. Our proposed FMR method is a novel method, because by employing fuzzy logic we were able to control the contrast enhancement in l space, as well as the color co-efficients were controlled in $\alpha\beta$ space in order to alleviate the fade color effect at a certain level. Many researchers had employed NMF, ICA to solve this problem of color variation in histopathology images. However, all those methods had large computation complexity compared to our proposed method. Subsequently, it was mathematically proved that proposed FMR method had satisfied all three hypotheses, the first hypothesis was not dependent on any parameters employed in the algorithm. However, second and third hypothesis were dependent on some parameters, which were fixed all over the database. Thus, performance of FMR method is not fluctuating over different databases and proposed FMR method will always satisfy all three hypotheses of color normalization. Furthermore, we verified those mathematical proofs with the experimental results of local quality metrics. We found that they were exactly correlated and our proposed method has the best quality metric values compared to other benchmark methods. Hence, we can conclude that our proposed FMR method has outperformed all other existing color normalization methods.

APPENDIX-I

A statistical analysis of Reinhard method is presented in this section.

By taking global variance both side in equation (12) and by employing the equation (28) we get,

$$\sigma_g^2(l_2) = \sigma_g^2\left[\mu_g(l_1)\right] + \left[\sigma_g^2(l) - \sigma_g^2(\mu_g(l_1))\right]. * \left[\sigma_g^2(l_1)/\sigma_g^2(l)\right] \quad (61)$$

Since, $\sigma_g^2(const) = 0$, equation (61) implies that,

$$\sigma_g^2(l_2) = \sigma_g^2(l_1) \quad (62)$$

or,

$$\sigma_g(l_2) = \sigma_g(l_1) \quad (63)$$

By taking the global mean both side in equation (12),

$$\mu_g(l_2) = \mu_g\left[\mu_g(l)\right] + \left[\mu_g(l) - \mu_g(\mu_g(l))\right]. * \left[\sigma_g^2(l_1)/\sigma_g^2(l)\right] \quad (64)$$

or,

$$\mu_g(l_2) = \mu_g(l_1) \quad (65)$$

Similarly, in α-β space, we can get the equations (66) and (67).

$$\mu_g(a_2) = \mu_g(a) \quad (66)$$

$$\mu_g(b_2) = \mu_g(b) \quad (67)$$

Equation (66) and (67) implies that global mean color (or background color) of target image is exactly same as mean color of the processed image. Thus, Reinhard algorithm satisfies the second hypothesis of color normalization.

By substituting value from equation (63) and (65) into equation (34),

$$C_2 = \frac{\sigma_g(l_2)}{\mu_g(l_2)} = \frac{\sigma_g(l)}{\mu_g(l)} \quad (68)$$

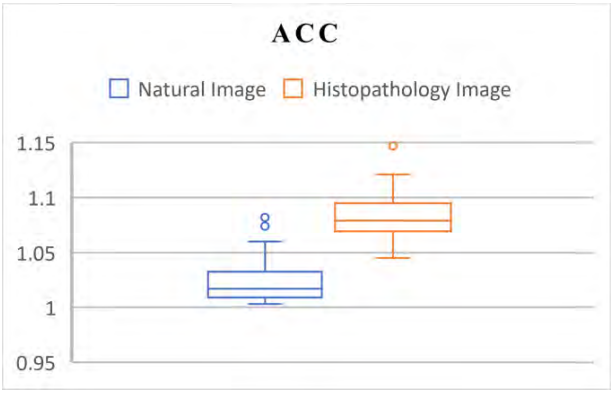

FIGURE 7. Box plot of ACC for natural image and histopathology images.

Equation (68) reveals that the global contrast (in l space) of the processed image is exactly equal to the global contrast of the target image by Reinhard method. If we have a source image, having higher contrast than that of target image, then also equation (68) hold true, thus, the processed image will have lesser contrast than that of target image. Therefore, Reinhard method doesn't satisfy the third hypothesis of color normalization.

To prove the first hypothesis, we have to prove that correlation co-efficient between source image and processed image will be equal to 1, by Reinhard method.

Substituting value from equation (65) and (12) into the covariance equation (36), we get,

$$\sigma_{ll_2} = \frac{1}{MN}\sum_{i=1}^{M}\sum_{j=1}^{N}\left[l_i - \mu_g(l_i)\right]^2 .* \left[\sigma_g(l_1)/\sigma_g(l)\right] \tag{69}$$

or,

$$\sigma_{ll_2} = \sigma_g(l) * \sigma_g(l_1) \tag{70}$$

Now substituting the value from equation (63) and (70) into equation (39), we get,

$$\delta = 1 \tag{71}$$

Similarly, in $\alpha\beta$ space, it can also be proved that correlation coefficient between source and processed image is 1, since transformation function in all three channels ($l\alpha\beta$) are similar.

APPENDIX-II

The mathematical formula of auto-correlation co-efficient (ρ) is given in equation (72), inspired by the work in [21].

$$\rho = \frac{\frac{1}{(W_1W_2-1)}\sum_{m=-(\frac{W_1}{2}-1)}^{\frac{W_1}{2}-1}\sum_{n=-(\frac{W_2}{2}-1)}^{\frac{W_2}{2}-1} I(x,y) * I(x+m,y+n)}{(I(x,y))^2} \tag{72}$$

where $m\&n \neq 0$, here both m and n are assumed to be odd number, $W_1 \times W_2$ is window size. For both natural images and histopathology images, 18×22 window size is taken. This auto-correlation co-efficient (ρ), estimated in equation (72), is just the measurement of self-similarity of pixels for only one single window. Final auto-correlation co-efficient of entire image can be measured by the following equation (73).

$$\rho_{total} = \frac{1}{W}\sum_{i=1}^{W}\rho_i \tag{73}$$

where W is the total number of windows in image, ρ_i is the auto-correlation co-efficient, estimated for i^{th} window.

TABLE 4. Comparison of mean values of ACC between histopathology and natural image.

Mean value of ACC for 50 histopathology images	Mean value of ACC for 50 natural images
1.084	**1.024**

Mean values of Auto-Correlation Coefficients (ACC) of histopathology images and natural images are presented in the following table 4. 50 natural images are randomly captured from Cannon-power shot camera and 50 histopathology images are randomly taken from the liver [13] and breast [28] databases.

Table 4 reveals that autocorrelation co-efficient of histopathology images are greater than that of natural images. This can be better visualized by the boxplot diagram, shown in Fig.6. This is to clarify that ACC value of histopathology images is only 0.06 greater than that of natural images, this 6% deviation is significant. Because with respect to a complete homogeneous image (blank image, whose ACC=1), natural images' ACC value deviation is just 0.02. Thus, relative to that deviation (of 0.02), 0.06 is significant variation for histopathology images, according to our visualization. Therefore, this has been verified that auto-correlation co-efficient of histopathology images are more deviating (6% extra) from the value of 1, than the natural images. Closer the value of auto-correlation co-efficient to 1, implies that the image pixels intensity values have greater self-similarity. This reveals that, unlike natural images histopathology images do not have large homogeneous regions (like trees, sky, lands etc) where intensity values are mostly similar. Because of this unique texture property of histopathology images, global color transformation is actually preferable over local transformation. Furthermore, employing such a global transformation can reduce the computation complexity significantly.

REFERENCES

[1] M. N. Gurcan, L. E. Boucheron, A. Can, A. Madabhushi, N. M. Rajpoot, and B. Yener, "Histopathological image analysis: A review," *IEEE Rev. Biomed. Eng.*, vol. 2, no. 2, pp. 147–171, Feb. 2009.

[2] M. T. McCann, "Tools for automated histology image analysis," M.S. thesis, Dept. Biomed. Eng., Carnegie Mellon Univ., Pittsburgh, PA, USA, May 2015.

[3] M. T. McCann, J. A. Ozolek, C. A. Castro, B. Parvin, and J. Kovacevic, "Automated histology analysis: Opportunities for signal processing," *IEEE Signal Process. Mag.*, vol. 32, no. 1, pp. 78–87, Jan. 2015.

[4] F. Ghaznavi, A. Evans, A. Madabhushi, and M. Feldman, "Digital imaging in pathology: Whole-slide imaging and beyond," *Annu. Rev. Pathol., Mech. Disease*, vol. 8, pp. 331–359, Jan. 2013.

[5] S. Roy, A. K. Jain, S. Lal, and J. Kini, "A study about color normalization methods for histopathology images," *Micron*, vol. 114, pp. 42–62, Nov. 2018.
[6] A. Vahadane *et al.*, "Structure-preserving color normalization and sparse stain separation for histological images," *IEEE Trans. Med. Imag.*, vol. 35, no. 8, pp. 1962–1971, Aug. 2016.
[7] X. Li and K. N. Plataniotis, "A complete color normalization approach to histopathology images using color cues computed from saturation-weighted statistics," *IEEE Trans. Biomed. Eng.*, vol. 62, no. 7, pp. 1862–1873, Jul. 2015.
[8] A. Janowczyk, A. Basavanhally, and A. Madabhushi, "Stain normalization using sparse autoencoders (StaNoSA): Application to digital pathology," *Comput. Med. Imag. Graph.*, vol. 57, pp. 50–61, Apr. 2017.
[9] N. Alsubaie, "Stain deconvolution using statistical analysis of multi-resolution stain colour representation," *PLoS ONE*, vol. 12, p. e0169875, Jan. 2017, doi: 10.1371/journal.pone.0169875.
[10] A. C. Ruifrok and D. A. Johnston, "Quantification of histochemical staining by color deconvolution," *Anal. Quant. Cytol. Histol.*, vol. 23, no. 4, pp. 291–299, Aug. 2001.
[11] A. Rabinovich, S. Agarwal, C. A. Laris, J. H. Price, and S. Belongie, "Unsupervised color decomposition of histologically stained tissue samples," in *Advances in Neural Information Processing Systems*. Cambridge, MA, USA: MIT Press, 2003.
[12] M. Macenko *et al.*, "A Method for normalizing histology slides for quantitative analysis," in *Proc IEEE Int. Symp. Biomed. Imag.*, Jun./Jul. 2009, pp. 1107–1110.
[13] A. M. Khan, N. Rajpoot, D. Treanor, and D. Magee, "A nonlinear mapping approach to stain normalization in digital histopathology images using image-specific color deconvolution," *IEEE Trans. Biomed. Eng.*, vol. 61, no. 6, pp. 1729–1738, Jun. 2014.
[14] M. T. McCann, J. Majumdar, C. Peng, C. A. Castro, and J. Kovacevic, "Algorithm and benchmark dataset for stain separation in histology images,"in *Proc. IEEE Int. Conf. Image Process.*, Oct. 2014, pp. 3953–3957.
[15] M. Gavrilovic *et al.*, "Blind color decomposition of histological images," *IEEE Trans. Med. Imag.*, vol. 32, no. 6, pp. 983–994, Jun. 2013.
[16] P. A. Bautista, N. Hashimoto, and Y. Yagi, "Color standardization in whole slide imaging using a color calibration slide," *J. Pathol. Inform.* vol. 5, p. 4, Jan. 2014.
[17] B. E. Bejnordi *et al.*, "Stain specific standardization of whole-slide histopathological images," *IEEE Trans. Med. Imag.*, vol. 35, no. 2, pp. 404–415, Feb. 2016.
[18] E. Reinhard, M. Adhikhmin, B. Gooch, and P. Shirley, "Color transfer between images," *IEEE Comput. Graph. Appl.*, vol. 21, no. 5, pp. 34–41, Sep./Oct. 2001.
[19] R. C. Gonzalez and R. E. Woods, *Digital Image Processing*, 2nd ed. Upper Saddle River, NJ, USA: Prentice-Hall, 2002.
[20] M. T. McCann, D. G. Mixon, M. C. Fickus, C. A. Castro, J. A. Ozolek, and J. Kovacevic, "Images as occlusions of textures: A framework for segmentation," *IEEE Trans. Med. Imag.*, vol. 23, no. 5, pp. 2033–2046, May 2014.
[21] R. M. Haralick, "Statistical and structural approaches to texture," *Proc. IEEE*, vol. 67, no. 5, pp. 786–804, May 1979.
[22] Z. Wang and A. C. bovik, "A Universal image quality index," *IEEE Signal Process. Lett.*, vol. 9, no. 3, pp. 81–84, Mar. 2002.
[23] A. Papoulis and S. U. Pillai, *Probability, Random Variables, and Stochastic Processes*, 2nd ed. Upper Saddle River, NJ, USA: Prentice-Hall, 2002.
[24] Z. Wang, A. C. Bovik, H. R. Sheikh, and E. P. Simoncelli, "Image quality assessment. From error visibility to structural similarity," *IEEE Trans. Image Process.*, vol. 13, no. 4, pp. 600–612, Apr. 2004.
[25] T. Celik and T. Tjahjadi, "Contextual and variational contrast enhancement," *IEEE Trans. Image Process.*, vol. 20, no. 12, pp. 3431–3441, Dec. 2011.
[26] D. L. Ruderman, T. W. Cronin, and C.-C. Chiao, "Statistics of cone responses to natural images. Implications for visual coding," *J. Opt. Soc. Amer. A, Opt. Image Sci.*, vol. 15, no. 8, pp. 2036–2045, 1998.
[27] Z. Gui and Y. Liu, "An Image sharpening algorithm based on fuzzy logic," *Optik*, vol. 122, pp. 697–702, Apr. 2010.
[28] L. Roux *et al.*, "Mitosis detection in breast cancer histological images," *J. Pathol. Inform.*, vol. 4, no. 8, pp. 1–8, 2013.
[29] J. Mukherjee and S. K. Mitra, "Enhancement of color images by scaling the DCT coefficients," *IEEE Trans. Image Process.*, vol. 17, no. 10, pp. 1783–1794, Oct. 2008.
[30] C. Mosquera-Lopez, R. Escobar, and S. Agaian, "Modeling human-perceived quality for the assessment of digitized histopathology color standardization," in *Proc. IEEE Int. Conf. Imag. Syst. Techn.*, Sep. 2015, pp. 1–6, doi. 10.1109/IST.2015.7294526.
[31] M. Frigge, D. C. Hoaglin, and B. Iglewicz, "Some implementations of the boxplot," *Amer. Statist.*, vol. 43, no. 1, pp. 50–54, Feb. 1989.

SANTANU ROY received the M.Tech. degree in information and communication technology from the Dhirubhai Ambani Institute of Information and Communication Technology, Gandhinagar, India, in 2011. He is currently pursuing the Ph.D. degree with the National Institute of Technology Karnataka, Surathkal, India. His current research interests include image processing, machine learning, histopathology image analysis, and computer-aided detection of cancer cells from histopathology images.

SHYAM LAL received the Ph.D. degree in digital image processing from the Department of Electronics and Communication Engineering, Birla Institute of Technology at Mesra, Ranchi, Jharkhand, India, in 2013. He has been an Assistant Professor with the Department of Electronics and Communication Engineering, National Institute of Technology Karnataka, Mangalore, Karnataka, India, since 2013. He has more than 16 years of teaching and research experience. He has supervised three Ph.D. students, and five Ph.D. students are currently working under his supervision in the area of medical and remote sensing image processing. He has published more than 61 research papers in the area of digital image processing, medical image processing, and remote sensing in international/national journals and at conferences. His research interests include digital image processing, histopathology image processing, medical image processing, remote sensing image processing, application of deep learning, and optimization algorithms in digital image processing. He is a Senior Member of IEEE, a Life Member of ISTE, New Delhi, India, a Life Member of IAENG, Hong Kong, and a Life Member of IACSIT, Singapore. He received the Early Career Research Award (Young Scientist) from the Science Engineering and Research Board, Department of Science and Technology, Government of India, in 2017, and the Young Faculty Research Fellowship Research Grant under the Visvesvaraya Ph.D. Scheme for Electronics and IT, MEITY, Government of India, in 2018. He has been a Guest Editor of IJSISE (Inderscience Publishers) and an Editorial Member of the *Open Access Journal of Biomedical Engineering and Its Applications* (Lupine Publishers, USA). He has supervised three doctoral students in the area of image processing.

JYOTI R. KINI received the M.D. degree in pathology from the Department of Pathology, Kasturba Medical College at Mangalore, Manipal Academy of Higher Education, Manipal, Karnataka, India, where she is currently an Associate Professor. She has more than 18 years of teaching and research experience. She has published more than 12 research papers in the area of histopathology, cytopathology, and hematology in international/national journals and at conferences. Her research interests include histopathology, cytopathology, and hematology.